Environmental Science Nano

Accepted Manuscript

ROYAL SOCIETY OF CHEMISTRY

rsc.li/es-nano

Environmental Science
Nano

Cite this: DOI: 10.1039/c0xx00000x

ARTICLE TYPE

www.rsc.org/xxxxxx

Surface functional groups and defects on carbon nanotubes affects adsorption-desorption hysteresis of metal cations and oxoanions in water

Jie Li[a,b], Changlun Chen[a,*], Shouwei Zhang[a] and Xiangke Wang[a,b,*]

Received Xth XXXXXXXXX 2014,

Accepted Xth XXXXXXXXX 2014
DOI: 10.1039/b000000x

This study investigated the influence of structure characteristics of carbon nanotubes (CNTs), such as surface oxygen-containing functional groups, specific surface area (SSA) and concentration of defects, on adsorption-desorption hysteresis of a metal cation (Cu(II)) and two oxoanions (As(V) and Cr(VI)) from single, double and multi-walled CNTs (SWCNTs, DWCNTs and MWCNTs), and two oxidized MWCNTs with different oxygen concentration (MWCNTs-O1, 2.51 wt% O and MWCNTs-O2, 3.5 wt% O). Oxygen-containing functional groups contributed to an increase in adsorption capacity for Cu(II) from aqueous solution, while a decrease for Cr(VI) and As(V). The sequence of adsorption capacity based on CNT SSA was MWCNTs-O2 > MWCNTs-O1 > MWCNTs > DWCNTs > SWCNTs, which was consistent with the sequence of CNT defect content. The desorption hysteresis index (HI) values for Cu(II) increased as functional groups increased. For Cr(VI) and As(V), however, HI values decreased as functional groups increased. HI values decreased with increasing metal ion surface coverage on CNTs. A shift in metal ion adsorption mechanisms by CNTs may be from more irreversible to more reversible processes with the increase in adsorbed metal ions. The understanding of the desorption hysteresis of heavy metal ions is important and useful for application and risk assessment of CNTs in the natural environment.

Nano impact

The understanding of the adsorption-desorption hysteresis of metal cations and anions from CNTs is important and useful for the application and risk assessment of CNTs. This work probes the influence of structural properties, such as surface functional groups, specific surface area and concentration of defects, on the adsorption-desorption hysteresis of metal ions by CNTs, and compares the difference in adsorption behavior and possible hysteresis phenomena of metal cation and anion ions.

Introduction

The potential applications of carbon nanotubes (CNTs) vary from power hand-held devices[1] to drug delivery,[2] flexible conductive thin films, cell regeneration and 3D scaffolds for tissue.[3,4] Because of their large specific surface area (SSA), hollow and layered structure, CNTs have already been investigated as promising sorbents for various organic pollutants and metal ions and radionuclides.[5-12] The increase in extensive applications and commercial interest of CNTs will result in subsequent mass production, thus causing greater possibility for interactions with environment and human beings.[13] Because of their small size, they can enter into cells, causing damage to plants, animals and humans,[14-16] the primary risk of CNTs originates from their toxicity. In addition, the toxicity of CNTs results from the adsorbed harmful pollutants.[17] To some extent, mobile CNTs may be also carry adsorbates to ecological or biological receptors, and CNTs can act effectively as a "Trojan Horse",[11] potentially transporting harmful pollutants to place that they cannot otherwise reach by adsorption and desorption. Metal ions play an important risk in ecosystems, but can also induce public health hazards, such as low blood pressure, diarrhea, paralysis, lung irritation and bone defects.[18] Therefore, it is necessary to consider the synergistic or antagonistic interactions of metal ions and CNTs so as to understand the toxicology and environmental impacts of CNTs for potential applications.

The study of adsorption-desorption behavior of harmful pollutants from CNTs is motivated by the need to understand the toxicity of CNTs and to assess potential environmental risks. As the reverse course of adsorption, desorption of toxic pollutants from CNTs makes harmful pollutants mobile and bioavailable in the aqueous environment, thus the toxicity of pollutants and

CNTs both remains.[19] Desorption hysteresis, which is generally shown with the desorption isotherm branch above the adsorption isotherm branch, includes reversible and irreversible hysteresis. Irreversible hysteresis indicates that a fraction of adsorbed pollutants remains on CNTs. Desorption hysteresis of organic pollutants from carbon nano-materials has been studied.[20-26]

According to CNT layers, there exist two distinct types of CNTs, single walled CNTs (SWCNTs) and multi-walled CNTs (MWCNTs). The outermost surface, inner cavities, interstitial channels, and grooves of CNTs constitute the four possible types of adsorption sites.[20] The adsorption capacity of CNTs will be affected by the physicochemical characteristics of CNTs (such as number of walls, surface functional groups, SSA and defects). CNTs are extremely hydrophobic and prone to aggregation as bundles. Aggregation results in a reduction in SSA, which is a potential negative impact for adsorption.[27] The interstitial channels and grooves on the periphery of the nanotube bundles, have a potential positive impact for more adsorption per mass.[28]

The surface functional groups on CNTs, such as carboxyl, phenol and lactone, affect the interaction with specific or polar adsorbates.[29] Defective sites within CNTs could be responsible for the sensitivity of nanotubes to adsorbates, thus affecting the adsorption ability of CNTs.[30] Zhang et al.[31] studied the adsorption behavior of aromatic compounds by CNTs and found that the adsorption capacity depended upon inner cavities and structure of CNT bundles. Wu et al.[20] proposed that adsorption behavior of organic compounds was closely related to oxygen-containing groups of CNTs. Feng et al.[32] found that ammonia was placed on top of the tube and in the vicinity of defect sites with the self-consistent charge density functional tight binding method. However, neither CNT surface area and surface functional groups, nor defects alone, can be applied to fully explain CNT adsorption characteristics. In order to understand the adsorption of metal ions by CNTs, their structural characteristics must be systematically considered in the analysis of the adsorption data. Up to now, little information on such analyses exists in the literature.[33] Comparison of the adsorption-desorption hysteresis of metal cations and anions from CNTs is scarce. Thus, in the context of both engineered water treatment and risk assessment of CNTs in the environment, the knowledge of adsorption-desorption hysteresis of metal cations and anions from CNTs is important and useful.

The objectives of this work are to probe the influence of structural properties, such as surface functional groups, SSA and defect contents, on the adsorption-desorption hysteresis of all three adsorbates (one cationic species (Cu(II) and two anionic species (anionic species of As(IV) and Cr(IV)) by CNTs from aqueous solution, and to compare the difference in adsorption behavior and possible hysteresis phenomena of metal cations and anions. Cu(II) was chosen as a model of metal cations. Cr(VI) and As(V) were selected as metal anions because they are both the most extremely toxic heavy metals. The existence of three metal ions in aquatic environments and their species distribution in solution were described in Supporting Information SI-1. On the basis of the prominent differences in the aqueous chemistry of the three metal ions, it was proposed that their adsorption and desorption behaviors would also be significantly different. To better understand the influence of structure properties of CNTs on the adsorption-desorption hysteresis of metal ions, we have combined our adsorption-desorption studies with surface characterization.

Experimental Details

Chemicals

Cu(II), Cr(VI) and As(V) stock solutions at 0.1 mol/L were prepared by $Cu(NO_3)_2$, $K_2Cr_2O_7$ and Na_2HAsO_4, which were purchased from Shanghai Chemical Reagent Co., Ltd. All received reagents were of analytical reagent grade and used without any further treatment. Milli-Q water (Millipore, Billerica, MA, USA) was used in all experiments.

Carbon nanotubes

SWCNTs, DWCNTs, MWCNTs and two oxidized MWCNTs with different oxygen concentrations (MWCNTs-O1, 2.51 wt% O and MWCNTs-O2, 3.5 wt% O) were applied in this study. The CNTs purchased from Beijing DK nano technology Co., Ltd. were prepared using Chemical Vapor Deposition (CVD) method and used as received. The ash contents of these five CNTs were determined via thermogravimetric analysis method. The Boehm titration method was carried out to determine the surface acidic groups (lactonic, hydroxyl and carboxyl groups, which is associated to the pH values) of the CNTs (see SI-2 of Supporting Information for details). Carbon atomic percentages and surface oxygen of the CNTs were calculated via X-ray photoelectron spectroscopy technique (see SI-3 of Supporting Information). SSA values of the CNTs were determined by the Brunauer-Emmett-Teller method (see SI-4 of Supporting Information). The surface chemistry of CNTs was further characterized by Raman spectroscopy performed at a wavelength of 514.57 nm (Ar^+) with an NR-1800 laser Raman spectrometer (JASCO, Japan). The determined properties of the CNTs were tabulated in Table 1.

Batch adsorption-desorption experiments

The adsorption of Cu(II), Cr(VI) and As(V) on the five types of CNTs was carried out in a 50 mL polyethylene centrifuge tube by batch technique. The system was adjusted to the desired concentrations of different components by adding stock suspensions of the CNTs and metal ions. The sonication was used in an attempt to disperse the nanotubes to suspensions. The desired pH was adjusted by adding negligible volumes of 0.01 or 0.1 mol/L HNO_3 or NaOH. The ionic strength (I) was fixed at 0.01 M using $NaNO_3$ as background. Preliminary kinetic study confirmed the adsorption equilibrium with the five types of CNTs was effectively completed for Cu(II), Cr(VI) and As(V) within 10 h (seen in Fig. S4). The suspensions were shaken by end-over-end rotation for 24 h to ensure that the adsorption equilibrium of Cu(II), Cr(VI) and As(V) were well achieved. The solid and liquid phases were separated by centrifugation at 18 000 rpm for 20 min. UV-vis absorption at 500 nm can be calibrated to CNT amount and used to determine full centrifugation of all CNTs in supernatant.[34] Detection limit was approximately 0.8 mg/L.

The Cu(II), Cr(VI) and As(V) concentrations were measured by atomic absorption spectrophotometry. After centrifugation, the adsorbed amounts of heavy metal ions were calculated from the difference between the initial (C_0) and equilibrium (C_e) concentration in the supernatant. Control experiments using metal ions in solution without CNTs showed that control centrifuge tubes adsorbed less than 2% of metal ions. The adsorption

percentage was calculated as: adsorption (%) = $(C_0 - C_e)/C_0 \times 100\%$.

Desorption experiments were carried out by substituting the supernatant with electrolyte solution without the metal ions of interest so as to reduce metal ion concentration in the solution phase. In detail, after the adsorption experiments, half of the supernatant was quickly removed and the equal volume of background electrolyte solution (0.01M $NaNO_3$) with the same pH value was injected into each centrifuge tube. At the same conditions as in the adsorption experiments, the suspension was shaken for 2 d. The desorption experiment procedures were repeated for a second circulation. All the adsorption-desorption experiments were carried out at 298 K.

Results and Discussion

pH influence

The pH influence on Cu(II), Cr(VI) and As(V) removal by the CNTs is given in Fig. 1. This is well known that the removal of metal ions by the CNTs highly depends on pH.[5-7,11] Fig. 1A shows that Cu(II) removal by the CNTs increases gradually as pH increases from 2.0 to 8.5, and finally keeps constant with increasing pH. However, Cr(VI) or As(V) adsorption decreases as pH increases from 1.0 to 8.0 (Fig. 1B and C). The ionization degree, speciation of surface functional groups and surface charges of the CNTs are affected by the solution pH. The zeta-potential of CNTs at different pH values is measured and shown in Fig. 1D. At acidic pH condition, surface functional groups (carboxyl, phenolic and lactonic) exist in solution in the protonated form. On the other hand, the functional groups on adsorbent surface exist in the deprotonated form at basic pH condition. These results are consistent with prior research and with Derjaguin-Landau-Verwey-Overbeek theory,[35-37] as explained through basic electrostatic interactions between charged surfaces and charged species in solution.

Cu(II) removal mechanism mainly involves ionic attraction between Cu^{2+}, $Cu_2(OH)_2^{2+}$, $Cu(OH)^+$, $Cu(OH)_2$, $Cu(OH)_3^-$ and $Cu(OH)_4^{2-}$ species (Fig. S1A) and the surface functional groups of adsorbents. The decrease in competition between Cu(II) ions and proton for the functional groups of CNTs and increase in negative surface charge result in the increase of Cu(II) adsorption as pH increases. Cu(II) concentration in solution is no longer controlled by adsorption at pH > 8.5 where the precipitation occurs. However, Cr(VI) or As(V) adsorption decreases as pH increases from 1.0 to 8.0, which can be relevant to the Cr(VI) or As(V) speciation in solution and the ionic state and type of functional groups on the surface of CNTs. At pH below the electrostatic point of CNTs, electrostatic attraction between positively charged adsorbent surface and negatively charged $HCrO_4^-$ or $H_2AsO_4^-$ (Figs. S1B and S1C) results in higher adsorption. At high pH, the reduction in Cr(VI) and As(V) adsorption contributes to the electrostatic repulsion and the competition for the effective adsorption sites of metal anions with the OH^-. At pH 4.0, the order of adsorption efficiency for $HCrO_4^-$ or $H_2AsO_4^-$ was MWCNTs > DWCNTs > SWCNTs > MWCNTs-O1 > MWCNTs-O2.

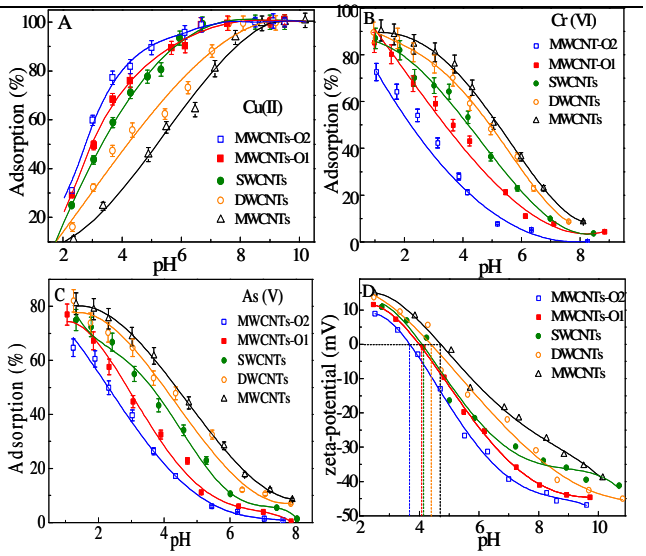

Fig. 1 Heavy metal ion adsorption on the CNTs as a function of pH, Cu(II) (A), Cr(VI) (B) and As(V) (C), at $C_{Cu\ initial}$ = 0.15 mmol/L, $C_{Cr\ initial}$ = $C_{As\ initial}$ =0.05 mmol/L, m/V = 1.0 g/L, I = 0.01M $NaNO_3$, T = 298 K and zeta-potential (D) of SWCNTs, DWCNTs, MWCNTs, MWCNTs-O1 and MWCNTs-O2.

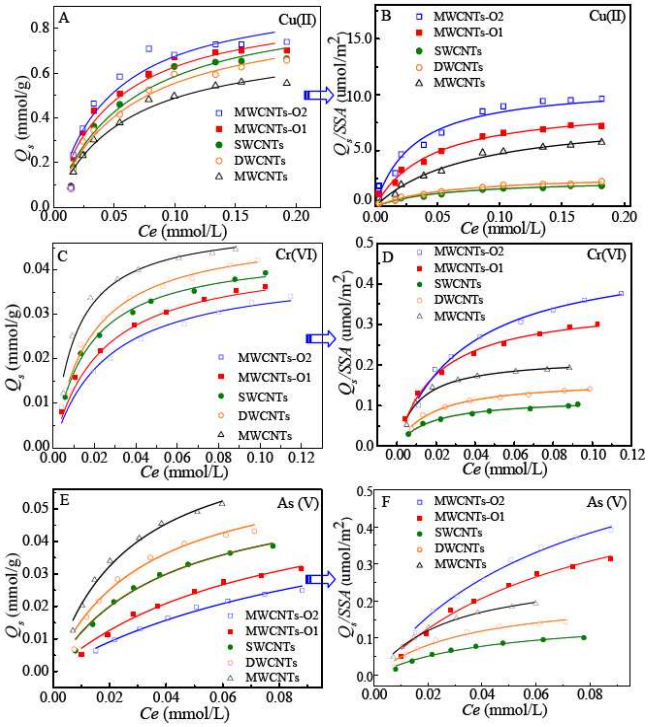

Fig. 2 Adsorption isotherms of Cu(II) (A, B) at pH = 5.0, Cr(VI) (C, D) and As(V) (E, F) at pH = 4.0, on the CNTs. m/V = 1.0 g/L, I = 0.01M $NaNO_3$ and T = 298 K. Dots represent the experimental data and fitting lines represent the Langmuir model.

Adsorption isotherms

The adsorption isotherms for Cu(II), As(V) and Cr(VI) by the CNTs are shown in Fig. 2. The Langmuir plots are also represented and the regression data are shown in Table S2. From Fig. 2A and Table S2, the adsorption capacities for Cu(II) on the base of adsorbent mass follow a tread of MWCNTs-O2 >

MWCNTs-O1 > SWCNTs > DWCNTs > MWCNTs. Similar result was reported by Cho et al.[11], indicating that Zn(II) and Cd(II) adsorption on MWCNTs increased with increasing the content of oxygen-containing functional groups. From Figs. 2C, 2E and Table S2, the trend of adsorption capacities for As(V) and Cr(VI) was observed as: MWCNTs-O2 < MWCNTs-O1 < SWCNTs < DWCNTs < MWCNTs, which clearly showed a systematic decrease in the extent of As(V) and Cr(VI) adsorption with increasing content of total functional groups in CNTs. The trend is exactly opposite of the cations. For metal anions, more functional groups (such as -COOH and -OH) are not conducive to As(V) and Cr(VI) adsorption due to electrostatic repulsion between deprotonation oxygen-containing functional groups and negatively charged $HCrO_4^-$ or $H_2AsO_4^-$. Similar finding was also observed in the adsorption of Cr(VI) onto functionalized and non-functionalized MWCNTs.[38] This phenomenon was in good agreement with Cr(VI) removal by oxidized activated carbon.[39] Park and Jang [40] also showed that the adsorption of Cr(VI) onto a carbon surface decreased in the presence of oxygen surface complexes.

From Table 1, the SSA values for SWCNTs, DWCNTs, MWCNTs, MWCNTs-O1 and MWCNTs-O2 are 380.1, 299.5, 101.8, 90.7 and 78.6 m^2/g, respectively. Both SSA and surface defect have positive influence on CNT adsorption capacity. It is useful to consider the influence of SSA by comparing *Qs* after surface area normalization. For this purpose, the SSA-normalized adsorption capacity (*Qs*/SSA) is applied to evaluating the influence of CNT surface defects and shown in Figs. 2B, 2D and 2F. A consistent sequence of CNT *Qs*/SSA for Cu(II), As(V) and Cr(VI) is obtained: MWCNTs-O2 > MWCNTs-O1 > MWCNTs > DWCNTs > SWCNTs.

It has been hypothesized that the structural defects within CNTs could serve as nucleating sites, thus affecting the adsorption ability of CNTs.[41] Experimental results and theoretical studies showed that NH_3 adsorption on SWCNT surfaces was sensitive to the functionalities and defects.[25] Raman spectroscopy has been a sensitive probe of the electronic structure in CNTs and presence of defects.[42] The D band in graphite at around 1300 cm^{-1} involves scattering from a defect which breaks the basic symmetry of the graphene sheet, it is observed in sp^2 carbons containing porous, impurities or other symmetry-breaking defects. The changes in the *D* band of Raman spectra can be used for materials characterization to probe and monitor structural modifications of the nanotube sidewalls that originate from the introduction of defects and the attachment of different chemical species. When estimating the defect concentration, the D mode intensity is usually normalized with respect to the intensity of the G mode at around 1600 cm^{-1}.[43] This approach relies on the assumption that the intensity of the G mode is independent of defect concentration and originates from a single resonant Raman process. The comparison of the ratios of these two peaks intensities gives a measure of the quality of the bulk samples. The relative relationship between the D band and G band is the key. In general, the ratio of the D and G band intensities (I_D/I_G) is used to measure the structural defect concentrations of CNTs.[44,45] If both bands have similar intensity, this indicates a high quantity of structural defects.[46]

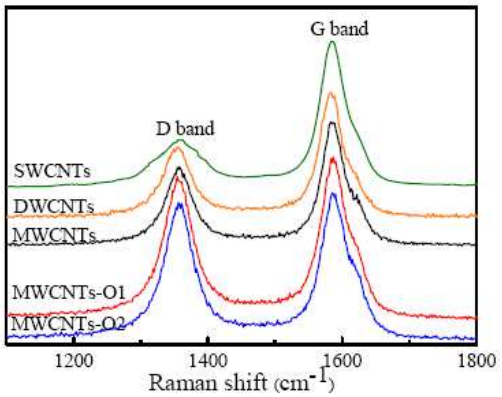

Fig. 3 Raman spectra of SWCNTs, DWCNTs, MWCNTs, MWCNTs-O1 and MWCNTs-O2.

In this study, Raman modes have been analyzed to testify the defective nature of the CNTs and shown in the frequency range 1100–1800 cm^{-1} (Fig. 3). The different I_D/I_G values of SWCNTs, DWCNTs, and MWCNTs can be explained as follows: Defects such as vacancies and dangling bonds may be formed during the growth of CNTs, especially using CVD due to high temperature. With increasing the wall number of CNTs, the I_D/I_G values increases. MWCNTs exhibit a higher quantity of structural defects due to their multiple graphite layers and intershell structural defects compared with SWCNTs and DWCNTs.[47]

In addition, the additional oxygen-containing groups in MWCNTs-O1 and MWCNTs-O2 will behave as covalent bonding-like defects. The counted I_D/I_G values are 0.39, 0.59, 0.64, 0.88 and 0.94 for SWCNTs, DWCNTs, MWCNTs, MWCNTs-O1 and MWCNTs-O2, respectively (Table 1). Therefore, the sequence of the CNT defect concentration follows: MWCNTs-O2 > MWCNTs-O1 > MWCNTs > DWCNTs > SWCNTs, which is in good agreement with the adsorption capacities per unit SSA. It proves that the lattice defects, which cause the so-called acceptor-like ''localized states'',[46] may be one of the factors which result in adsorption ability of CNTs. CNT defects have positive effect on Cr(VI) and As(V) adsorption, while the deprotonation oxygen-containing functional groups of CNTs have negative effect on Cr(VI) and As(V) adsorption. The introduction of oxygen-containing functional groups can produce more surface defects, so it is difficult that the importance of charge and surface defects is disentangled. For our case, the sequence of the CNT defect concentrations is in good agreement with the adsorption capacity per unit SSA. The CNT surface defect contributions may overwhelm the negative effect of the deprotonation oxygen-containing functional groups on Cr(VI) and As(V) adsorption.

Adsorption-desorption hysteresis

Fig. 4 shows the adsorption-desorption hysteresis of heavy metal ions on or from CNTs, initiated by substituting the supernatant with electrolyte solution without metal ions. The adsorption isotherms of Cu(II), Cr(VI) and As(V) are observed below the desorption isotherms, and the first desorption isotherms are below the second desorption isotherms. From Figs. S4 and S5, the adsorption and desorption processes of Cu(II), Cr(VI) and As(V) significantly occurred in the initial rapid process and reached equilibrium within 2 d, the observed phenomenon was unlikely

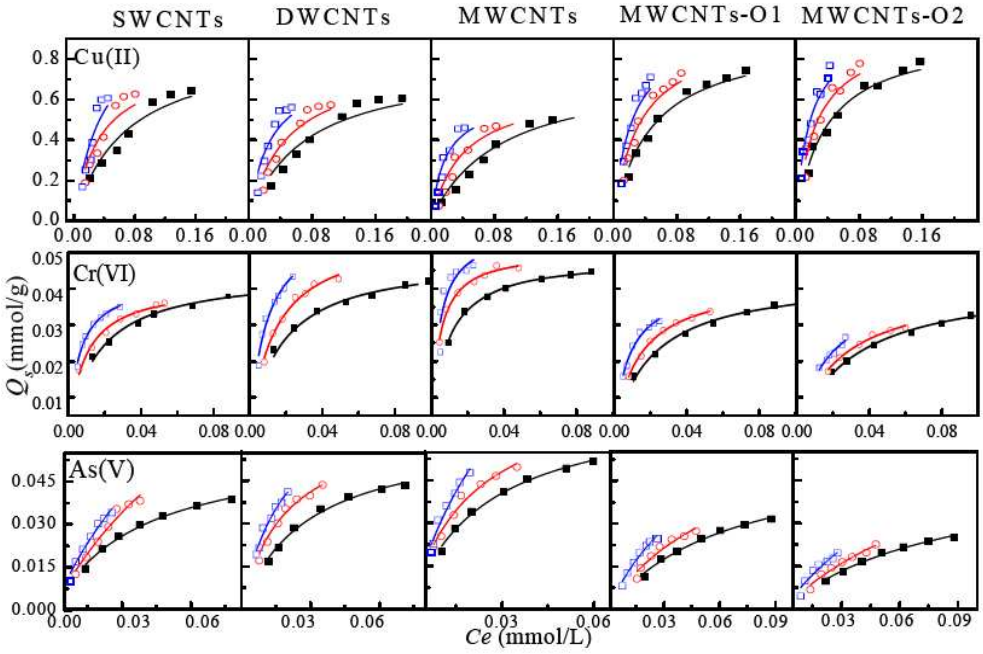

Fig. 4 Adsorption-desorption isotherms of Cu(II) (A, B) at pH = 5.0, Cr(VI) (C, D) and As(V) (E, F) at pH = 4.0, on the CNTs. m/V = 1.0 g/L, I = 0.01M $NaNO_3$ and T = 298 K. Solid square (■) represents the adsorption data, open (O) represents the first desorption data, open square (□) represents the second desorption data, and fitting lines represent the Langmuir model.

completely due to non-equilibrium state because the suspension in this study was shaken for 2 d. This phenomenon implies that irreversible reactions may exist in the adsorption processes. In some researcher reports,[21,24,26] deformation-rearrangement of the CNT aggregates and adsorbate penetration into the closed interstitial spaces of CNT bundles was proposed to explain the adsorption hysteresis of polycyclic aromatic hydrocarbons. However, Yang and Xing [21] reported that CNTs with long and cylindrical structure could not form closed interstitial spaces and thus could not result in desorption hysteresis for organic compounds. Hummer et al.[48] studied the adsorption of H_2O by uncapped SMCNTs and found that water molecules can enter the central channels of the nanotubes by forming hydrogen-bonded chains. The opinions in the literature were different and had not reached a uniform understanding. For our experiment, the sonication was used in attempts to disperse the nanotubes to suspensions and to reduce effect of large aggregates on metal ion adsorption. In our earlier study of desorption kinetics of Am(III) bound to MWCNTs using chelating resin. The results clearly proved the existence of strong chemical binding of Am(III) to the nanotubes.[5] The experimental results indicated that Am(III) formed kinetically stabile complexes with MWCNTs and did not rapidly desorb into the solution. Two types of adsorption complexes for Am(III) on MWCNTs, one of strong complexation and the other of weak complexation, which provided the 'readily desorbed' and 'less readily desorbed' fractions of Am(III), respectively.

A adsorption-desorption hysteresis index (HI, Equations 1 and 2)[20] was used to standardize the gap between adsorption and desorption branches of the isotherms as follows:

$$HI_1 = (Q_e^{d1} - Q_e^s)/Q_e^s\big|_{T,Ce} \quad (1)$$

$$HI_2 = (Q_e^{d2} - Q_e^s)/Q_e^s\big|_{T,Ce} \quad (2)$$

where Q_e^s, Q_e^{d1} and Q_e^{d2} all in millimole per gram are the equilibrium concentrations of solid phase for adsorption, the first desorption and second desorption procedures, respectively. The subscripts T (kelvins) and C_e (millimole per liter) indicate the temperature constants and residual solution phase concentration of metal ions. As shown in Table 2, CNTs have a lower HI values at higher metal ion surface coverage. However, HI values increase, when metal ion surface coverage decreases. A shift in the metal ion adsorption mechanism may be from more irreversible to more reversible processes with the increase in adsorbed metal ions. In addition, HI_2 values are generally higher than HI_1. Heavy metal ions may be irreversibly adsorbed on high-energy sites at low metal ion loading. Moreover, HI values of Cu(II) on CNTs increase with the amount of surface functional groups on the CNT surface increases. However, HI values for anions (As(V) and Cr(VI)) on CNTs decrease as functional groups increase, which is in good agreement with the decrease of adsorption capacity of the CNTs for anions with the increase in functional groups. It is evident from HI values that adsorption-desorption hysteresis varies for different metal ions, but also that they appear to correlate with the chemical characteristics of related metal ions and CNTs.

Conclusions

The oxygen-containing functional groups contributed to an increase in adsorption capacity for Cu(II), while a decrease for Cr(VI) and As(V). The adsorption capacity based on CNT SSA increased with the increase in CNT defect content. The HI values for cations (such as Cu(II)) increased as the oxygen-containing functional groups increased. However, for anions (such as Cr(VI) and As(V)), HI values decreased as the oxygen-containing functional groups increased. HI values decreased with increasing metal ion surface coverages on CNTs. A shift in metal ion adsorption mechanisms by CNTs may be from more irreversible to more reversible processes with the increase in adsorbed metal ions. The immobilization of metal ions may originate from the irreversible formation of surface complexes and nucleation. The desorption hysteresis and irreversible immobilization of metal ions on CNTs will influence their mobility and bioavailability, and consequently their toxicity will be altered in the environment. Therefore, the desorption hysteresis and irreversible immobilization of metal cations and anions on different CNTs and the toxicity change should be studied for detailed risk assessment of metal ions and CNTs in the natural environment.

Acknowledgements

Financial supports from NSFC (91126020, 41273134, 91326202, 21225730), Chinese National Fusion Project for ITER (NO. 2013GB110000), Hefei Center for Physical Science and Technology (2012FXZY005), and the Priority Academic Program Development of Jiangsu Higher Education Institutions, the Collaborative Innovation Center of Radiation Medicine of Jiangsu Higher Education Institutions are acknowledged.

Notes and references

[a] *Key Laboratory of Novel Thin Film Solar Cells, Institute of Plasma Physics, Chinese Academy of Sciences, P.O. Box 1126, Hefei, 230031, P.R. China*

[b]*School for Radiological and Interdisciplinary Sciences (RAD-X), Soochow University, Suzhou 215123, P.R. China*

Tel: +86-551-65592788 Email: clchen@ipp.ac.cn (C. L. Chen); xkwang@ipp.ac.cn (X.K. Wang)

† Electronic Supplementary Information (ESI) available: More details about heavy metal ion specie distribution, Boehm titration, XPS survey spectra of CNTs, BET data of CNTs, adsorption and desorption kinetics, and the Langmuir model fitted results to adsorption-desorption. See DOI: 10.1039/b000000x/

1 F. S. Gittleson, D. J. Kohn, X. Li and A. D. Taylor, *ACS Nano*, 2012, **6**, 3703−3711.
2 Z. Liu, K. Chen, C. Davis, S. Sherlock, Q. Z. Cao, X. Y. Chen and H. J. Dai, Cancer Res., 2008, **68**, 6652−6660.
3 D. Movia, A. Prina-Mello, D. Bazou, Y. Volkov and S. Giordani, *ACS Nano*, 2011, **5**, 9278−9290.
4 M. A. Correa-Duarte, N. Wagner, J. Rojas-Chapana, C. Morsczeck, M. Thie and M. Giersig, *Nano Lett.,* 2004, **4**, 2233−2236.
5 X. K. Wang, C. L. Chen, W. P. Hu, A. P. Ding, D. Xu and X. Zhou, *Environ. Sci. Technol*., 2005, **39**, 2856−2860.
6 C. L. Chen, J. Hu, D. Xu, X. L. Tan, Y. D. Meng and X. K. Wang, *J. Colloid Interface Sci.,* 2008, **323**, 33−41.
7 C. L. Chen and X. K. Wang, *Ind. Eng. Chem. Res.,* 2006, **45**, 9144−9149.
8 R. Q. Long and R. T. Yang, *J. Am. Chem. Soc.,* 2001, **123**, 2058−2059.
9 X. L. Wang, J. L. Lu and B. S. Xing, *Environ. Sci. Technol.,* 2008, **42**, 3207−3212.
10 K. Yang, L. Z. Zhu and B. S. Xing, *Environ. Sci. Technol.,* 2006, **40**, 1855−1861.
11 H. H. Cho, K. Wepasnick, B. A. Smith, F. K. Bangash, D. H. Fairbrother and W. P. Ball, *Langmuir*, 2010, **26**, 967–981.
12 H. H. Cho, B. A. Smith, J. D. Wnuk, D. H. Fairbrother and W. P. Ball, *Environ. Sci. Technol.* **2008,** *42,* 2899–2905.
13 S. Kang, M. Herzberg and D. F. Rodrigues, *Langmuir*, 2008, **24**, 6409−6413.
14 N. W. S. Kam, T. C. Jessop, P. A. Wender and H. J. Dai, *J. Am. Chem. Soc.,* 2004, **126**, 6850−6851.
15 Q. Lu, J. M. Moore, G. Huang, A. S. Mount, A. M. Rao, L. L. Larcom and P. C. Ke, *Nano Lett.,* 2004, **4**, 2473−2477.
16 S. Foley, C. Crowley, M. Smaihi, C. Bonfils, B. F. Erlanger, P. Seta and C. Larroque, *Biochem. Biophys. Res. Commun.,* 2002, **294**, 116−119.
17 Y. L. Zhao, G. M. Xing and Z. F. Chai, *Nature Nanotechnol*., 2008, **3**, 191−192.
18 D. C. Adriano, Trace elements in terrestrial environments: biogeochemistry, bioavailability, and risks of metals. Springer. New York, 2001.
19 J. Zhao, Z. Y. Wang, H. Mashayekhi, P. Mayer, B. Chefetz and B. S. Xing, *Environ. Sci. Technol.,* 2012, **46**, 5369−5377.
20 W. H. Wu, W. Jiang, W. D. Zhang, D. H. Lin and K. Yang, *Environ. Sci. Technol*., 2013, **47**, 8373−8382.
21 K. Yang and B. S. Xing, *Environ. Pollut.,* 2007, **145**, 529−537.
22 X. K. Cheng, A. T. Kan and M. B. Tomson, *J. Nanopart. Res.,* 2005, **7**, 555−567.
23 X. B. Wang, Y. Q. Liu, W. F. Qiu and D. B. Zhu, *J. Mater. Chem.* 2002, **12**, 1636−1639.
24 B. Pan, D. H. Lin, H. Mashayekhi and B. S. Xing, *Environ. Sci. Technol.,* 2008, **42**, 5480−5485.
25 P. Oleszczuk, B. Pan and B. S. Xing, *Environ. Sci. Technol*., 2009, **43**, 9167−9173.
26 Z. Y. Wang, X. D. Yu, B. Pan and B. S. Xing, *Environ. Sci. Technol.,* 2010, **44**, 978−984.
27 S. J. Zhang, T. Shao, S. S. K. Bekaroglu and T. J. Karanfil, *Environ. Sci. Technol.,* 2009, **43**, 5719–5725.
28 J. J. Zhao, A. Buldum, J. Han and J. P. Lu, *Nanotechnology,* 2002, **13**, 195–200.
29 Y. H. Li, S. G. Wang, Z. K. Luan, J. Ding, C. L. Xu and D. H. Wu, *Carbon*, 2003, **41**, 1057−1062.
30 L. Valentini, L. Lozzi, S. Picozzi, C. Cantalini, S. Santucci and J. M. Kenny, *J. Vac. Sci. Technol.,* 2004, **22**, 1450−1454.
31 S. J. Zhang, T. Shao, H. S. Kose and T. karanfil, *Environ. Sci. Technol.,* 2010, **44**, 6377−6383.
32 X. Feng, S. Irle, H. Witek, K. Morokuma, R. Vidic and E. Borguet, *J. Am. Chem. Soc.,* 2005, **127**, 10533–10538.
33 J. Li, C. L. Chen, S. W. Zhang, X. M. Ren, X. L. Tan and X. K. Wang, *Chem. Asian J.,* 2014, **9**, 1144–1151.
34 B. Smith, K. Wepasnick, K. E. Schrote, H. H. Cho, W. P. Ball and D. H. Fairbrother, *Langmuir,* 2009, **25**, 9767-9776.
35 N. B. Saleh, L. D. Pfefferle and M. Elimelech, *Environ. Sci. Technol.* 2008**, 42***,* 7963–7969.
36 B. Smith, K. Wepasnick, K. E. Schrote, A. R. Bertele, W. P. Ball, C. O'Melia and D. H. Fairbrother, *Environ. Sci. Technol.*, 2009, **43**, 819–825.
37 M. Sano, J. Okamura and S. Shinkai, *Langmuir*, 2001, **17**, 7172–7173.
38 K. Pillay, E. M. Cukrowska and N. J. Coville, *J. Hazard. Mater*., 2009, **166**, 1067−1075.
39 S. J. Park and Y. S. Jang, *J. Colloid. Interface Sci.,* 2002, **249**, 458–463.
40 G. Arslan and E. Pehlivan, *Bioresource Technol.,* 2007, **98**, 2836–2845.
41 B. C. Regan, S. Aloni, R. O. Ritchie, U. Dahmen and A. Zettl, *Nature,* 2004, **428**, 924–928.
42 M. Pimenta, G. Dresselhaus, M. S. Dresselhaus, L. Cancado, A. Jorio and R. Saito *Phys. Chem. Chem. Phys.* 2007, **9**, 1276–1290.
43 K. Jeet, V. K. Jindal, L. M. Bharadwaj, D. K. Avasthi and K. Dharamvir, *J. Appl. Phys.,* 2010, **108**, 034302.
44 W. Z. Qian, T. Liu, F. Wei and H. Y. Yuan, *Carbon* 2003, **41**, 1851–1854.
45 D. K. Singh, P. K. Giri and P. K. Iyer, *J. Phys. Chem. C,* 2011, **115**, 24067–24072.
46 M. S. Dresselhaus, G. Dresselhaus, R. Saito and A. Jorio, *Phys. Rep.* 2005, **409**, 47–99.
47 X. M. Shi, B. B. Jiang, J. D. Wang and Y. R. Yang, *Carbon*, 2012, **50**, 1005–1013.
48 G. Hummer, J. C. Rasaiah and J. P. Noworyta, *Nature (London),* 2001, **414**, 188–190.

Table 1 Selected properties of the CNTs

Adsorbents	SSA(m^2/g)	Purity (wt%)	I_D/I_G	Surface atom (wt%)		Surface acidic group content (mmol/g)			
				C	O	Hydroxyl	Carboxyl	Lactonic	Total
SWCNTs	380.1	> 95	0.39	98.9	1.1	0.00245	0.004301	0.01629	0.02304
DWCNTs	299.5	> 95	0.55	98.7	1.3	0.00237	0.003757	0.018893	0.02502
MWCNTs	131.8	> 95	0.67	99.2	0.8	0.00272	0.003632	0.015061	0.02141
MWCNTs-O1	90.7	> 95	0.88	97.4	2.6	0.06311	0.003967	0.004144	0.07122
MWCNTs-O2	78.6	> 95	0.94	96.5	3.5	0.02024	0.072151	0.011369	0.10376

Table 2 Desorption hysteresis indexes of heavy metal ions on the CNTs

CNTs	pH	HI_1		HI_2	
		0.005 mmol/L	0.03 mmol/L	0.005 mmol/L	0.03 mmol/L
			Cu(II)		
SWCNTs	5.0	0.10±0.01	0.05±0.01	0.20±0.01	0.09±0.02
DWCNTs	5.0	0.12±0.01	0.08±0.01	0.24±0.01	0.16±0.01
MWCNTs	5.0	0.14±0.02	0.10±0.01	0.26±0.02	0.18±0.01
MWCNTs-O1	5.0	0.16±0.01	0.12±0.01	0.27±0.01	0.20±0.01
MWCNTs-O2	5.0	0.27±0.04	0.14±0.01	0.38±0.02	0.22±0.01
			Cr(VI)		
SWCNTs	4.0	0.27±0.02	0.25±0.02	0.59±0.02	0.54±0.02
DWCNTs	4.0	0.22±0.01	0.18±0.02	0.53±0.01	0.48±0.01
MWCNTs	4.0	0.21±0.01	0.17±0.01	0.43±0.02	0.36±0.01
MWCNTs-O1	4.0	0.16±0.01	0.14±0.02	0.37±0.03	0.32±0.03
MWCNTs-O2	4.0	0.08±0.01	0.07±0.01	0.27±0.01	0.24±0.02
			As(V)		
SWCNTs	4.0	0.17±0.02	0.15±0.02	0.54±0.03	0.51±0.02
DWCNTs	4.0	0.15±0.02	0.14±0.02	0.48±0.02	0.46±0.02
MWCNTs	4.0	0.14±0.01	0.13±0.02	0.35±0.01	0.31±0.02
MWCNTs-O1	4.0	0.12±0.01	0.11±0.01	0.33±0.01	0.28±0.02
MWCNTs-O2	4.0	0.07±0.02	0.06±0.01	0.27±0.01	0.22±0.01

HI_1 and HI_2 represent hysteresis indexes of the first and second desorption cycle, respectively.

Environmental Science
Nano

Cite this: DOI: 10.1039/c0xx00000x

www.rsc.org/xxxxxx

ARTICLE TYPE

TOC

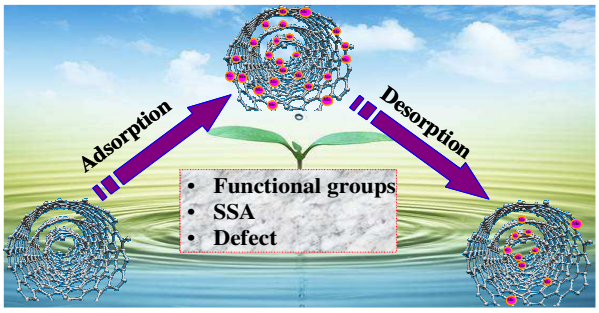

This study probed the effect of functional groups, SSA and defects on metal ion adsorption and desorption